Published in final edited form as:
Biomed Signal Process Control. 2008 October ; 3(4): 319–326. doi:10.1016/j.bspc.2008.04.005.

Adaptive Bolus Chasing Computed Tomography Angiography:

Control Scheme and Experimental Results

Zhijun Cai[1], **Colbin Erdahl**[1], **Kai Zeng**[2], **Tom Potts**[1], **Melhem Sharafuddin**[3], **Osama Saba**[4], **Ge Wang**[5], and **Er-Wei Bai**[1]

[1]Department of Electrical and Computer Engineering, University of Iowa, Iowa City, IA, 52242

[2]Department of Biomedical Engineering, University of Iowa, Iowa City, IA, 52242

[3]University of Iowa Hospital and Clinic, University of Iowa, Iowa City, IA, 52242

[4]Siemens Medical Solutions, Iowa City, IA, 52242

[5]VT-WFU School of Biomedical Engineering & Sciences, Virginia Polytechnic Institute & State University, Blacksburg, VA 24061, USA

Abstract

In this paper, a new adaptive bolus-chasing control scheme is proposed to synchronize the bolus peak in a patient's vascular system and the imaging aperture of a computed tomography (CT) scanner. The proposed control scheme is theoretically evaluated and experimentally tested on a modified Siemens SOMATOM Volume Zoom CT scanner. The first set of experimental results are reported on bolus-chasing CT angiography using realistic bolus dynamics, real-time CT imaging and adaptive table control with physical vasculature phantoms. The data demonstrate that the proposed control approach tracks the bolus propagation well, and clearly outperforms the constant-speed scheme that is the current clinical standard.

Keywords

Adaptive bolus chasing; Computed Tomography Angiography

I. Introduction

With the advent of the multi-slice CT scanner, CT Angiography (CTA) has become an important investigative tool for vascular diseases such as aneurysms and atherosclerosis [1-4]. It produces cross-sectional images of arteries throughout the body in a fast and minimally invasive way. To better define the vasculature from its surrounding soft tissue, a dose of contrast medium (a bolus) is usually injected into a vein through an IV (intravenous) tube. During the scanning, the patient lies on the CT table. The table is translated into the CT gantry, and the part of the patient's body which is under the x-ray aperture is scanned at that time. In the meantime, the contrast bolus propagates along the blood vessel. Consequently, synchronization of the CT imaging aperture and the contrast bolus peak would result in CT images with a higher Contrast to Noise Ratio (CNR).

The problem, however, is that the contrast bolus dynamics are highly nonlinear, complicated, and influenced by many factors, e.g., patient weight, vasculature diseases, and injection patterns. In current practice, the CT table moves at a preset constant speed, and is very likely to miss the bolus peak. To compensate for this problem, a large amount of contrast medium is injected, which is harmful to the patient's kidney.

To overcome the above problem, the timing bolus [5-7] and ROI (Region Of Interest) threshold triggering [8] methods have been proposed for a long time. Both methods endeavor to provide a "correct" time to start the CT table. The former method uses a small amount of the test contrast bolus to obtain the bolus arrival time at the ROI, which is then used to start the CT table for the normal scan. However, the arrival time for the test bolus and the main bolus may not be consistent because of different injection volumes and complicated bolus dynamics. The latter method presets a threshold for a selected ROI, and starts to move the CT table when the bolus density inside the ROI reaches this threshold. This is also questionable because the optimal threshold is not known a priori. When the threshold is set too low, the CT table starts too early, and when it is set too high, the CT table does not start at all. A fundamental problem for both methods is that they move the CT table at a constant velocity which does not match the varying bolus velocity during the propagation.

Another class of approaches to obtain the high-CNR CT images tries to optimize the bolus geometry by means of varying the injection rate and duration [8-15]. It is expected that if a bolus keeps its maximum density for a longer time at a position, then it is easier to synchronize the CT imaging aperture and the bolus peak. As a result, many injection protocols were reported. The multiple-injection method [15] injects the bolus at varying rates; the inverse method [16] obtains the injection protocol (input) from the desired output (the optimized bolus geometry) by taking the system as a LTI (Linear Time-Invariant) system. These approaches need a test bolus and/or a LTI system assumption, which is far away from the reality. In addition, the geometry optimization method may end up with a larger amount of contrast dose, which is not good for patients.

To make it clear, in the following texts "bolus chasing" means to track the bolus throughout the scan by means of varying the table speed, not just to chase the bolus arrival. The bolus chasing techniques were studied in Digital Subtraction Angiography (DSA) [17,18] and Magnetic Resonance Angiography (MRA) [19-22]. Preferable results have been reported in these studies. However, there are few studies on bolus chasing CTA [23]. The reason for this is that CTA has a much smaller field of view (z direction) compared to DSA or MRA, and the CT image reconstruction algorithm for varying pitch is complicated.

Recently, we have developed the CT image reconstruction algorithms for varying pitch [24] and investigated the bolus characteristic from hundreds of clinical bolus datasets [26]. We have also developed an adaptive bolus chasing control schemes and numerically tested it on clinical bolus datasets [25]. To the best of our knowledge, no experimental result has ever been reported in the literature on bolus chasing CTA. In this paper, we report the experimental results of the control schemes on a Siemens SOMATOM Volume Zoom CT scanner. Although the experiments are conducted on phantoms, results have successfully shown that the proposed control scheme works very well.

The layout of the paper is as follows. Bolus propagation model and problem statement are introduced in Section II. Section III describes the experimental setup. Section IV presents the approach to the problem. Then in Section V, the experimental results are given. Conclusions are provided in Section VI.

II. Bolus propagation model and problem statement

In this section, we discuss the bolus propagation model and formally state the bolus chasing problem.

Bolus propagation model

After the injection, the contrast bolus propagates and disperses in the blood vessel. Its density varies with time and distance (*z* direction). Due to the limited FOV (Field Of View) of CTA, it is not practical to obtain the bolus density information over a long distance. Many researchers have described the bolus using temporal profiles at several positions, such as the aorta and the liver [9,10,27]. Blomley and Dawson [28] suggested a Gamma function to depict the bolus time-attenuation profile at the aorta, and earlier, Stow and Hetzel [29] proposed an empirical formula for the bolus temporal curve. Probably the most well known temporal profile is the lagged normal density model reported by Bassingthwaighte in [30]. This model is able to fit the bolus curve for a wide range of cases. In our previous work [25], we fitted the bolus data to the lagged normal density model for a wide range of cases in the aorta, and as a result and we were able to obtain the bolus velocity in the aorta according to those profiles.

Although there are many models to describe the bolus temporal behavior at a position, a common property is that the bolus time-density curve is more or less like a bell for a single injection [9,10,25]. In other words, the bolus density is monotonically increasing and decreasing before and after reaching its maximum density, respectively. Based on this feature, we have designed an optimal adaptive control scheme for bolus chasing CTA [26]. The numerical simulation results based on the clinical data have shown that the adaptive bolus chasing control scheme outperforms the constant speed method substantially.

Problem statement

The control objective is to keep the peak of the moving bolus right under the x-ray aperture. This is achieved by instantaneously processing the bolus CT image on the monitor, dynamically predicting the bolus peak position at the next sampling time, and adaptively moving the CT table in the opposite direction to follow the bolus peak.

III. Experimental setup

In this section, the experimental setup is introduced, and some key parts are elaborated. Figure 1 is a photo of the experimental setup. The pump system, plastic tube filled with water and reservoirs are all placed on the CT table and used to simulate the blood system. When the pump is turned on, it drives the bolus inside the tube. The bolus velocity can be changed by varying the pump speed. During the scan, the bolus cross-sectional image is shown on the monitor by real time image reconstruction algorithms. A frame grabber is used to capture the CT images and feed the bolus information to the controller. The controller predicts the bolus peak position at the next sampling time, and sends a command to move the table accordingly. Thus, the bolus peak is kept right under the CT imaging aperture.

CT scanner

The CT scanner is a Siemens SOMATOM Volume Zoom four-slice CT scanner with software version A40A. Table 1 shows some critical technical parameters:

Siemens has also provided us with the CANbus access and command format in order to control the CT table.

Frame grabber

Although we have the CT reconstruction algorithm for varying pitch, we are not able to reconstruct the CT images due to the unavailability of the proprietary raw data. Therefore, the only possible feedback of the bolus density is the real time CT image on the monitor. To that end, we split the CT VGA signal, feed it to the controller, and capture it using a frame grabber. The frame grabber, manufactured by the NCast Corporation (http://www.ncast.com/DigiCaptureCard.html), is a Digitizer 3.0 Capture Card. It supports standard VGA input modes with a frequency of up to 85Hz and a maximum resolution of 1280× 1024, and is able to capture the image signal at a speed of 30 frames per second.

Pump system

The blood vascular system is physically simulated by a programmable MasterFlex pump system (HV-07523-60 L/S Brushless Digital Drives, made by the Cole Parmer Company, http://www.masterflex.com) connected to a plastic tube filled with water. By changing the pump head size and speed, the water flow rate can be varied between 0.6 and 3400 mL/min. During the experiment, we adjust the pump speed to achieve the desirable bolus dynamics. Roughly speaking, the bolus speed is proportional to the pump flow rate, though in reality it is not exactly proportional because of the irregularity of the tube and discontinuity of the flow.

Delay issues

As mentioned before, we have limited access to the CT scanner, which gives us two delays: an image display delay and a control delay. The image display delay is caused by the image reconstruction and display on the monitor. In this experiment, we used the CAREVision mode, and the image display delay is about 0.79 seconds. That is to say that when a target is sent into the CT gantry right under the x-ray aperture, its CT image will be shown on the monitor 0.79 seconds later. The other delay is the control delay, which is actually a combination of two delays caused by CANbus communication and table movement execution. In the CT CANbus system provided by Siemens, the CANbus decodes and encodes at rate of 100Kbps and takes a minimum of 100ms for transmitting or receiving a command. The table movement execution delay is the time needed to move the CT table from one position to another, and that depends on the length and speed of the movement. The combined delay is variable depending on the CANbus activity, the speed at which the controller can process the data, and the number of data bits in the message. To that end, we must wait for a certain time (CANbus command delay plus table moving time) between two consecutive CANbus commands, or the CT scanner would abandon the current scan and jump out of CAREVison mode. We have measured that the CANbus command delay is about 0.15 seconds on this CANbus system. The combined delay can be as high as 1.3-2 seconds. The translation is that once a control command is fed to the CANbus, the next control command can only be sent out after 1.3-2 seconds. This poses a very serious challenge for controller design. It is important to comment that the combined control delay is caused by the CANbus. If the full proprietary control commands are available to us, the control delay problem is nonexistent. We are currently working with Siemens to try to have those full proprietary control commands in the near future. All the results reported in this paper are under the control delay constraint.

IV. Approach

Ideally, we would like to be able to send CT table control commands continuously so that the CT table can follow the bolus peak continuously. Because of the delays, especially the significant control delay, the ability to follow a bolus with arbitrary dynamics is severely limited. Therefore, in the presence of a control delay, the bolus dynamics, including the maximum speed and the maximum acceleration, have to be scaled down to within the constraints imposed by the delays. Scaling down the bolus speed and acceleration can be done

easily by simply changing the pump flow. However, scaling down the bolus dispersion is not possible. To this end, in our experiments, we use a solid aluminum bolus immersed in the water instead of the actual liquid bolus. The temporal profile of the solid bolus is made to resemble the actual bell-shaped bolus. The dispersed bolus density is represented by the solid bolus cross-sectional area, and the bolus peak position is the center of the solid bolus. The basic idea of bolus chasing is to combine image feedback and control. The feedback information of the bolus dynamics is obtained from imaging reconstruction algorithms and is then used to guide the control. The experiment using a solid bolus should serve its purpose, i.e., it should be able to tell whether the idea of combining imaging and control is feasible. In fact, tracking a solid bolus with the length of about 40mm can actually be tougher than tracking a liquid bolus. A bolus about 40mm long is easily missed by the x-ray aperture if the CT table does not follow the bolus peak closely. Once missed, it is very hard to re-capture it because no feedback information on the bolus is available. On the other hand, because of dispersion, a liquid bolus is much longer and relatively easy to follow.

We now design a simple yet effective algorithm to track the bolus peak with the presence of the delays. The following notations will be used throughout the paper.

T_k	$T_k = k\Delta T$, where ΔT is the time interval between two consecutive control commands.
$Z(k)$	Table position at time T_k.
$B(k)$	Bolus peak position at timeT_k.
$E(k)$	Error between table position and bolus peak at time T_k, $E(k) = B(k) - Z(k)$.
α	Control gain.
Den(k)	Observed bolus density at time T_k.
l	Number of steps in the length of the display delay.

Assuming that the display delay is $l\Delta T$ which means that at time $T_k=k\Delta T$, the controller only has the bolus peak information up to time $(k\text{-}l)\Delta T$. The next CT table position $Z(k+1)$ is predicted as the combination of three components: 1) the current position of the CT table $Z(k)$, which is available; 2) the difference between the two consecutive bolus peak positions at times $(k\text{-}l)\Delta T$ and $(k\text{-}l\text{-}1)\Delta T$; and 3) the calculated error between the bolus peak position and the CT table position at time $(k\text{-}l)\Delta T$. Theorem 1 states the control law for the case when the bolus moves linearly.

Theorem 1

If the bolus is bell shaped as discussed above and moves at a constant speed, i.e., $B(k)=B(k\text{-}1)+\Delta$, for some constant $\Delta>0$, consider the following control law for some integer $l>0$,

$$Z(k+1) = Z(k) + [B(k-l) - B(k-l-1)] + \alpha E(k-l), \tag{1}$$

where $E(k)=B(k)\text{-}Z(k)$. Then, there exists $\alpha_{\max}(l)>0$, such that for all $0<\alpha<\alpha_{\max}(l)$, the closed loop system is exponentially stable, or equivalently, the error $E(k)$ goes to zero asymptotically.

Proof

The error dynamics are given as

$$\begin{aligned} E(k+1) &= B(k+1) - Z(k+1) = B(k+1) - Z(k) - [B(k-l) - B(k-l-1)] - \alpha E(k-l) \\ &= (B(k) + \Delta) - Z(k) - \Delta - \alpha E(k-l) \\ &= E(k) - \alpha E(k-l). \end{aligned}$$

The characteristic equation is

$$Z^{l+1} - Z^{l} + \alpha = 0.$$

Then for each integer l, there exists $\alpha_{\max}(l)>0$ so that for all $0<\alpha<\alpha_{\max}(l)$ the closed loop system is exponentially stable, which implies $\lim_{k\to\infty} E(k) \to 0$.■

Theorem 2 characterizes the performance of the control law when the bolus moves in a nonlinear fashion. The proof is similar and is omitted.

Theorem 2

Suppose the bolus is bell shaped as discussed and $B(k)=B(k\text{-}1)+\Delta_k$, and $|\Delta_i\text{-}\Delta_{i\text{-}l}|\leq \varepsilon$, for $\forall$ $1\leq i\leq l$. Then, considering the control law (1) with the same control gainα, the tracking error of the closed loop system is bounded by

$$|E(k)| \leq \gamma(\alpha)\,\varepsilon.$$

Since the image display delay is much smaller than ΔT, which is determined by the control delay, l=1 in all our experiments. The results, however, apply equally to any integer l.

Bolus profile and tracking error

To determine the tracking error in control law (1), we first obtain the bolus density profile before the experiment, and then approximate it by a 2nd order polynomial. The tracking error is obtained through the approximated polynomial and the online scanned density. To determine the bolus profile, we scan the bolus under the CAREVision mode (the same mode to implement the controller), and set the CT window center and width as 1500 Hounsfield Units (HU) and 500 HU, respectively. Thus, only the bolus is shown on the screen, because the aluminum has a CT number greater than 2000 HU, and the background is black. The bolus inside the plastic tube is fed into the gantry with water driven by the pump at a speed of 1mm/sec, and at the same time, the bolus CT images are captured by the frame grabber every 0.15 seconds. Thus, we can extract the bolus density from the VGA signal, which has a range of 0~255. Recall that our settings of the CT window center and width make the bolus almost white with a black background. Therefore, the bolus cross-sectional area is white on the screen. Further, we denote the bolus density by the number of pixels that are greater than a threshold. The threshold value is set to be 50 in order to account for all the pixels of the bolus. Figure 2 shows the bolus density profile. Let $Z_{\max}$ and $Z_{\min}$ be the bolus maximum and minimum positions in the z direction, and Z_c denote the bolus center or peak position. The bolus density at any position z can be approximated by

$$\mathrm{Den}(z) = \begin{cases} A(z - Z_c)^2 + C & Z_{\min} \leq z \leq Z_{\max} \\ 0 & z > Z_{\max} \quad \text{or} \quad z < Z_{\min} \end{cases}$$

where A and C are constants.

At time T_k, the table position is *Z(k)*, and the measured bolus density is Den (k)>0. Assume that the bolus center is *B(k)* at that time. By substituting *B(k)* for Z_c and *Z(k)* for *z*, we have

$$\text{Den}\,(k) = A(Z - (k) - B\,(k))^2 + C \tag{2}$$

Consequently, we are able to obtain the magnitude of the tracking error E(k) by

$$|E\,(k)| = |Z\,(k) - B\,(k)| = \sqrt{\frac{\text{Den}\,(k) - C}{A}}. \tag{3}$$

The next step is to determine the sign of the tracking error, because the observed density does not tell us whether the bolus center is ahead of or behind the x-ray aperture. A simple concept is shown in Figure 3. When the CT table is stopped, the bolus will be moving forward through the aperture. Thus, we will measure an increasing bolus density (Measurements 1 and 2) if the x-ray is scanning the head of the bolus (negative error). On the other hand, the decreasing measurement readings (Measurements 3 and 4) indicate that the bolus tail is being scanned (positive error). In practice, we take nine measurements, and determine the error sign by the slope of these densities to reduce the noise effect.

Remarks—

1. The table must be stopped while taking the measurements; otherwise the above argument is not valid. If the table moves faster in the opposite direction of the bolus, the error sign will be positive for measurements 1 and 2, and negative for measurements 3 and 4. Besides this, the table has to be stopped after a move to ensure that the CANbus command has been completely executed.
2. At the peak of the bolus, the error sign can easily be determined erroneously in the presence of noise, because the bolus density is more or less flat there, and a small change affects the determination of the sign. Fortunately, in this scenario, the magnitude of the error is small, which results in little movement, and does not have a noticeable impact.

Control procedure

Figure 4 is the flow chart of the bolus chasing CTA control procedure. The controller starts when the observed bolus density exceeds some preset threshold. Unlike the constant speed method, in the bolus chasing method, the controller being activated does not mean that the CT table moves forward right away. The speed and length of the next table movement depend on the measured bolus density. The tracking procedure is over when the CT has scanned the prescribed length. This is consistent with current clinical practice, where a length is pre-defined before a CT examination [4].

Because of the delay issues, it is critical to guarantee that we measure the bolus density during the time that the table is temporally stopped, and there is enough waiting time between two consecutive commands. Figure 5 shows the time arrangement for table moving, waiting, and image delay in one step. In Figure 5, the table moving time in one step is 0.7 seconds, and the image capturing time is about 0.35 seconds. It is easy to see that image capturing commands are sent while the table is stopped.

Dealing with the stopped bolus

In reality, when the bolus meets an aneurysm, or in certain other situations, it may stay there for a while before it moves again. To that end, the control law has to be modified, because the static bolus produces almost the same measurements and could result in a wrong tracking direction. Fortunately, we know that when the bolus is stopped, the variance of density measurements is small (we take nine measurements for each step), while the moving bolus gives a very big variance. Therefore, we say that if the density variance is small and the average density is in some range, then the bolus is stopped, and we move the table to its peak.

Remarks—

1. It is not suggested to move a big step while the bolus has been detected to be stopped, because the table may move the bolus across its peak and give a wrong error sign.
2. To detect whether or not the bolus is stopped, we need to check if the average density is close to the maximum, because when we are tracking on the bolus peak, the variance is also very small.

V. Experimental results

The experimental parameters are in Table 2.

In order to show the controller's ability to track the bolus with different dynamics, we programmed the pump for three kinds of patterns: constant bolus speed, exponentially decreasing bolus speed, and piecewise constant bolus speed. It is important to emphasize that the pump speed only roughly represents the bolus velocity, which is not known exactly throughout the experiment.

Constant bolus speed

For this experiment, the pump is running at 150 rpm all the time. The tracking results are shown in Figure 6, where the top plot shows the CT table movement trajectory, and the bottom plot shows the observed density at each time. We can see that the CT table starts before the 10^{th} second, when the observed density exceeds the threshold. Most of the measured densities are greater than 2000, which is very close to the maximum. The reason that there are a couple of points that have a value less than 1500 is that the bolus does not move constantly in the plastic tube due to the irregularity of the tube and the discontinuous pump output flow. Although we mentioned that the bolus velocity is not available throughout the experiment, we can tell the bolus trajectory roughly from Figure. 6. If the scanned bolus density is very close to the maximum, it means that we are tracking the bolus center well.

Exponentially decreasing bolus speed

The actual bolus in a human body does not flow constantly inside the blood vessel. It is reported that the blood flows slower in the artery when it is further away from the heart. For a normal male adult, the average blood velocity in the aorta is about 27cm/sec, while it is around 10cm/sec in the common femoral artery. To this end, we reduce the pump speed while the bolus is moving. The pump speed obeys the equation $V_p(t)=(125\text{-}90)e^{-0.01t}+110$, where $V_p(t)$ is the pump speed with unit rpm.

Figure 7 shows the experimental results for tracking the bolus driven by exponentially decreasing speed. In Figure 7, the top plot is the table movement and the bottom plot gives the scanned bolus density at each time step. Again, most of the measured densities are greater than 1500. It is noted that the scanned bolus density is jiggling all the time. The reason for this is that the pump speed is decreasing all the time, and the bolus does not flow constantly at all.

However, the controller is able to track the bolus well even if the bolus flows nonlinearly, provided that the bolus speed does not change too much.

Variable bolus speed

The bolus may stay in the same place for a while and then move again in some cases, such as an aneurysm. To simulate that, we reduce the pump speed to stop/slow the bolus for some time. Figure 8 is the pump speed profile, which shows that the pump runs at 90 rpm between 35 and 60 seconds, and 150 rpm before and after that period. The tracking results are shown in Figure 9, where the top plot shows the CT table movement trajectory, and the bottom plot shows the observed density. It is noticeable that the controller tracks the bolus well even when it is almost static between 35 and 60 seconds.

To compare the adaptive chasing method with the current constant CT table speed method, we scan the bolus with two different constant table speeds: 4mm/s and 3.5 mm/s. As we expect, results are unsatisfactory (see the bottom plot of Figure 10). The CT table that moves at a constant speed of 4mm/s only catches the bolus at the very beginning, and loses the bolus after 40 seconds, while the table moving at 3.5mm/s catches the bolus thrice and only scans the bolus peak for a few seconds. To make a quantitative comparison, we compute the average scanned densities over the scanning duration for both the adaptive chasing method and the constant CT table speed method, along with their percentages of the maximum density (2500) as shown in Table 3. It is clear that the adaptive chasing method follows close to the bolus peak (88.5%), while the constant CT table methods have poor performances, 10.4% and 30.9% for 4mm/s and 3.5mm/s, respectively.

Based on the normalized scanned bolus density, we reconstruct the 3D plastic tubes, which represent blood vessels, and are shown in Figure 11, where the left, middle and right “blood vessels” are reconstructed using the data for the adaptive tracking method, the 4mm/s constant CT table method, and the 3.5 mm/s method, respectively. Obviously, the 3D “blood vessel” based on the adaptive tracking method is fully reconstructed, while the constant CT table speed methods do not show the whole “blood vessel”. The reason for this is that the adaptive chasing method scanned the “blood vessel” from the beginning to the end with the peak of the bolus of contrast, while the constant speed methods did not.

VI. Concluding remarks

In this paper, we proposed a control scheme to track the contrast bolus using the feedback from real time CT images. Although the experiments were conducted on phantoms, the experimental results have shown that 1) the proposed scheme tracks the bolus center well (88.5% of the peak density), despite the delays in the system; 2) the adaptive tracking method outperforms the constant table speed method by a factor of 2.8 or more.

It is the first experiment result reported as we are aware of for adaptive bolus chasing CTA. In the near future, we will replace the tube with more realistic vasculature phantom, and program the pump to have an output of the real human heart. Eventually, we will apply this adaptive tracking method on the patient in clinic who needs an exam of the Computed Tomography Angiography.

Reference

1. Fleischmann D, Hallett RL, Rubin GD. CT angiography of peripheral arterial disease. J Vasc Interv Radiol 2006;17(1):3–26. [PubMed: 16415129]

2. Ofer A, Nitecki SS, et al. Multidetector CT angiography of peripheral vascular disease: a prospective comparison with intraarterial digital subtraction angiography. AJR Am J Roentgenol 2003;180(3): 719–24. [PubMed: 12591682]
3. Chow LC, Rubin GD. CT angiography of the arterial system. Radiol Clin North Am 2002;40(4):729–49. [PubMed: 12171182]
4. Van Hoe L, Gryspeerdt S, et al. Spiral CT angiography. J Belge Radiol 1995;78(2):114–7. [PubMed: 7601813]
5. van Hoe L, Marchal G, et al. Determination of scan delay time in spiral CT-angiography: utility of a test bolus injection. J Comput Assist Tomogr 1995;19(2):216–20. [PubMed: 7890844]
6. Puls R, Knollmann F, et al. Multi-slice spiral CT: 3D CT angiography for evaluating therapeutically relevant stenosis in peripheral arterial occlusive disease. Rontgenpraxis 2001;54(4):141–7. [PubMed: 11883117]
7. Bae KT. Test-bolus versus bolus-tracking techniques for CT angiographic timing. Radiology 2005;236 (1):369–70. [PubMed: 15987987]author reply 370
8. Schweiger GD, Chang PJ, Brown BP. Optimizing contrast enhancement during helical CT of the liver: a comparison of two bolus tracking techniques. AJR Am J Roentgenol 1998;171(6):1551–8. [PubMed: 9843287]
9. Bae KT, Heiken JP, Brink JA. Aortic and hepatic peak enhancement at CT: effect of contrast medium injection rate--pharmacokinetic analysis and experimental porcine model. Radiology 1998;206(2): 455–64. [PubMed: 9457200]
10. Cademartiri F, van der Lugt A, et al. Parameters affecting bolus geometry in CTA: a review. J Comput Assist Tomogr 2002;26(4):598–607. [PubMed: 12218827]
11. Claussen CD, Banzer D, et al. Bolus geometry and dynamics after intravenous contrast medium injection. Radiology 1984;153(2):365–8. [PubMed: 6484168]
12. Kirchner J, Kickuth R, et al. Optimized enhancement in helical CT: experiences with a real-time bolus tracking system in 628 patients. Clin Radiol 2000;55(5):368–73. [PubMed: 10816403]
13. Kopka L, Rodenwaldt J, et al. Dual-phase helical CT of the liver: effects of bolus tracking and different volumes of contrast material. Radiology 1996;201(2):321–6. [PubMed: 8888218]
14. Rist C, Nikolaou K, et al. Contrast bolus optimization for cardiac 16-slice computed tomography: comparison of contrast medium formulations containing 300 and 400 milligrams of iodine per milliliter. Invest Radiol 2006;41(5):460–7. [PubMed: 16625109]
15. Rossi P, Baert A, et al. Multiple bolus technique vs. single bolus or infusion of contrast medium to obtain prolonged contrast enhancement of the pancreas. Radiology 1982;144(4):929–31. [PubMed: 7111749]
16. Fleischmann D, Hittmair K. Mathematical analysis of arterial enhancement and optimization of bolus geometry for CT angiography using the discrete fourier transform. J Comput Assist Tomogr 1999;23 (3):474–84. [PubMed: 10348458]
17. Fritschy P, Terrier F. Intravenous digital subtraction angiography of the lower extremities combined with step translation (2-field DSA). Rofo 1988;148(3):279–84. [PubMed: 2832892]
18. Wu, Z.; Qian, J. IEEE Workshop on Biomedical Image Analysis. Santa Barbara, CA: 1988. Real-time tracking of contrast bolus propagation in X-ray peripheral angiography.
19. Wang Y, Lee HM, et al. Bolus-chase MR digital subtraction angiography in the lower extremity. Radiology 1998;207(1):263–9. [PubMed: 9530326]
20. Kruger DG, Riederer SJ, et al. Dual-velocity continuously moving table acquisition for contrast-enhanced peripheral magnetic resonance angiography. Magn Reson Med 2005;53(1):110–7. [PubMed: 15690509]
21. Ho VB, Choyke PL, et al. Automated bolus chase peripheral MR angiography: initial practical experiences and future directions of this work-in-progress. J Magn Reson Imaging 1999;10(3):376–88. [PubMed: 10508299]
22. Hany TF, Carroll TJ, et al. Aorta and runoff vessels: single-injection MR angiography with automated table movement compared with multiinjection time-resolved MR angiography--initial results. Radiology 2001;221(1):266–72. [PubMed: 11568351]
23. Bennett J, Bai E, et al. A Preliminary Study on Adaptive Field-of-View Tracking in Peripheral Digital Subtraction Angiograph. J. of X-ray Science and Technology 2003;11:149–159.

24. Yu H, Ye Y, et al. A backprojection-filtration algorithm for nonstandard spiral cone-beam CT with an n-PI-window. Phys Med Biol 2005;50(9):2099–111. [PubMed: 15843739]

25. Cai Z, Stolpen A, et al. Bolus characteristics based on Magnetic Resonance Angiography. Biomed Eng Online 2006;5:53. [PubMed: 17044929]

26. Bai E-W, Cai Z, et al. An Adaptive Optimal Control Design for a Bolus Chasing Computed Tomography Angiography. IEEE Transction on Control System Technology. 2006

27. Qanadli SD, Mesurolle B, et al. Abdominal aortic aneurysm: pretherapy assessment with dual-slice helical CT angiography. AJR Am J Roentgenol 2000;174(1):181–7. [PubMed: 10628476]

28. Blomley MJ, Dawson P. Bolus dynamics: theoretical and experimental aspects. Br J Radiol 1997;70 (832):351–9. [PubMed: 9166070]

29. Stow RW, Hetzel PS. An empirical formula for indicator-dilution curves as obtained in human beings. J Appl Physiol 1954;7(2):161–7. [PubMed: 13211491]

30. Bassingthwaighte JB, Ackerman FH, Wood EH. Applications of the lagged normal density curve as a model for arterial dilution curves. Circ Res 1966;18(4):398–415. [PubMed: 4952948]

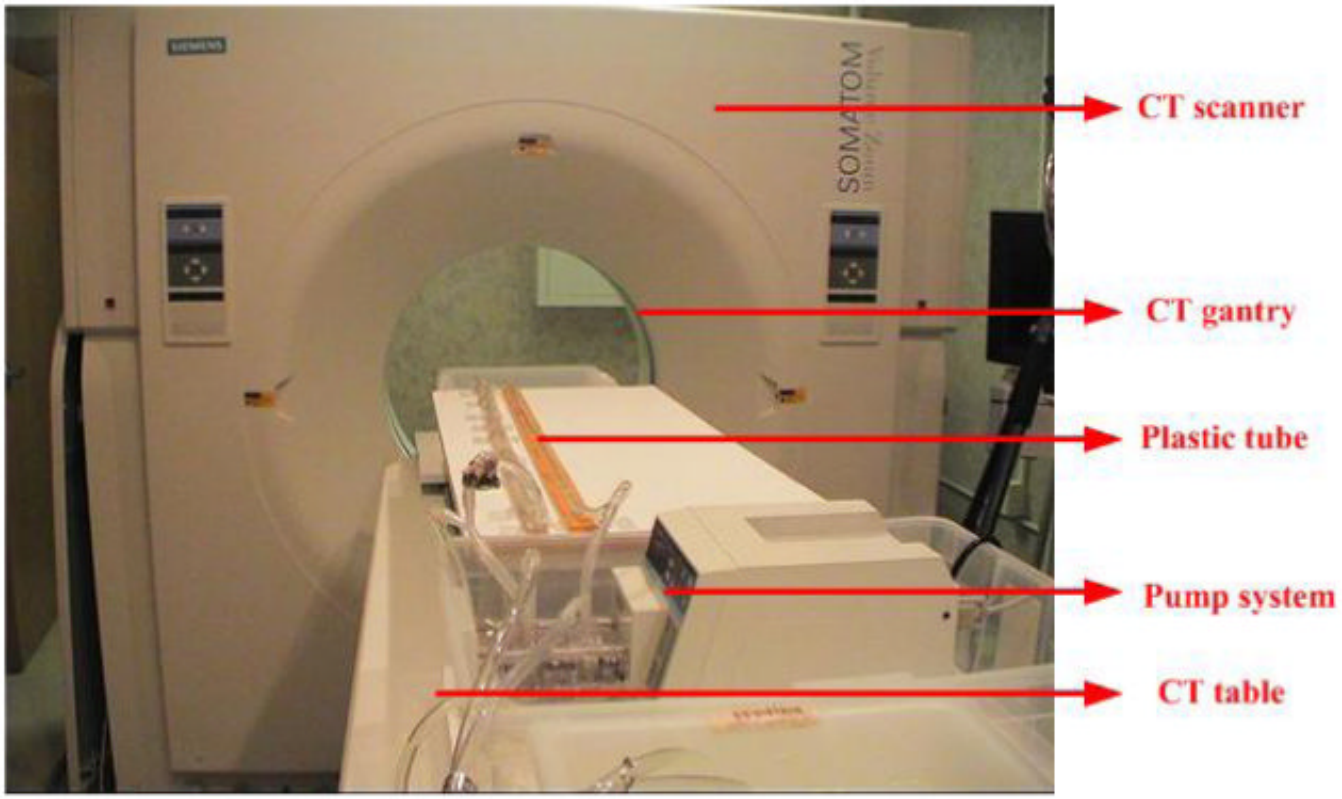

Figure 1. Experimental setup

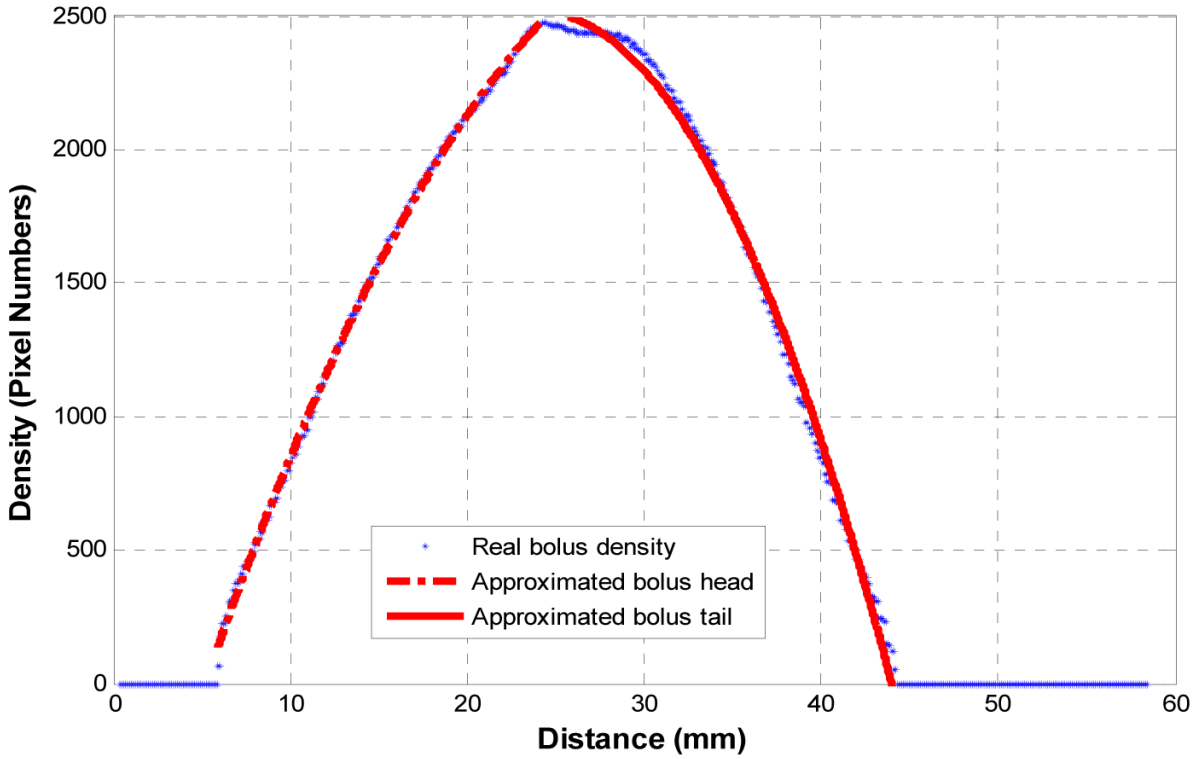

Figure 2. The bolus density profile and its 2nd order polynomial approximation

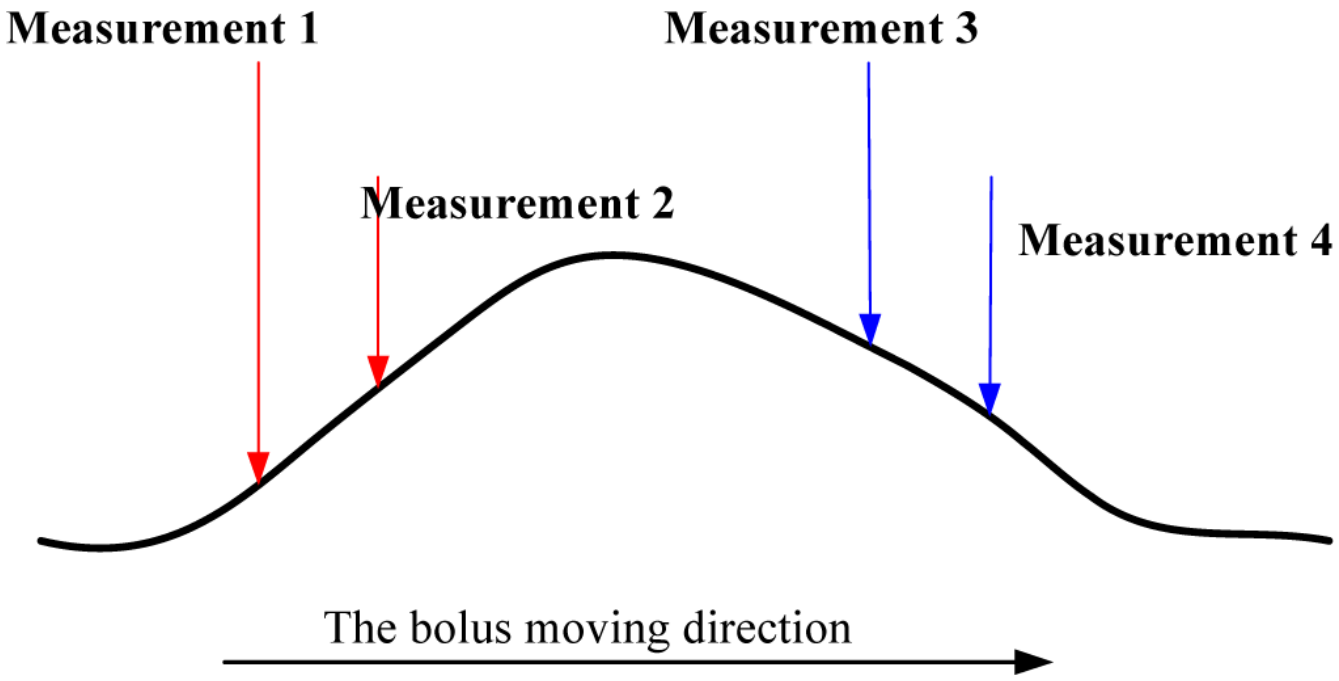

Figure 3. The slope determination

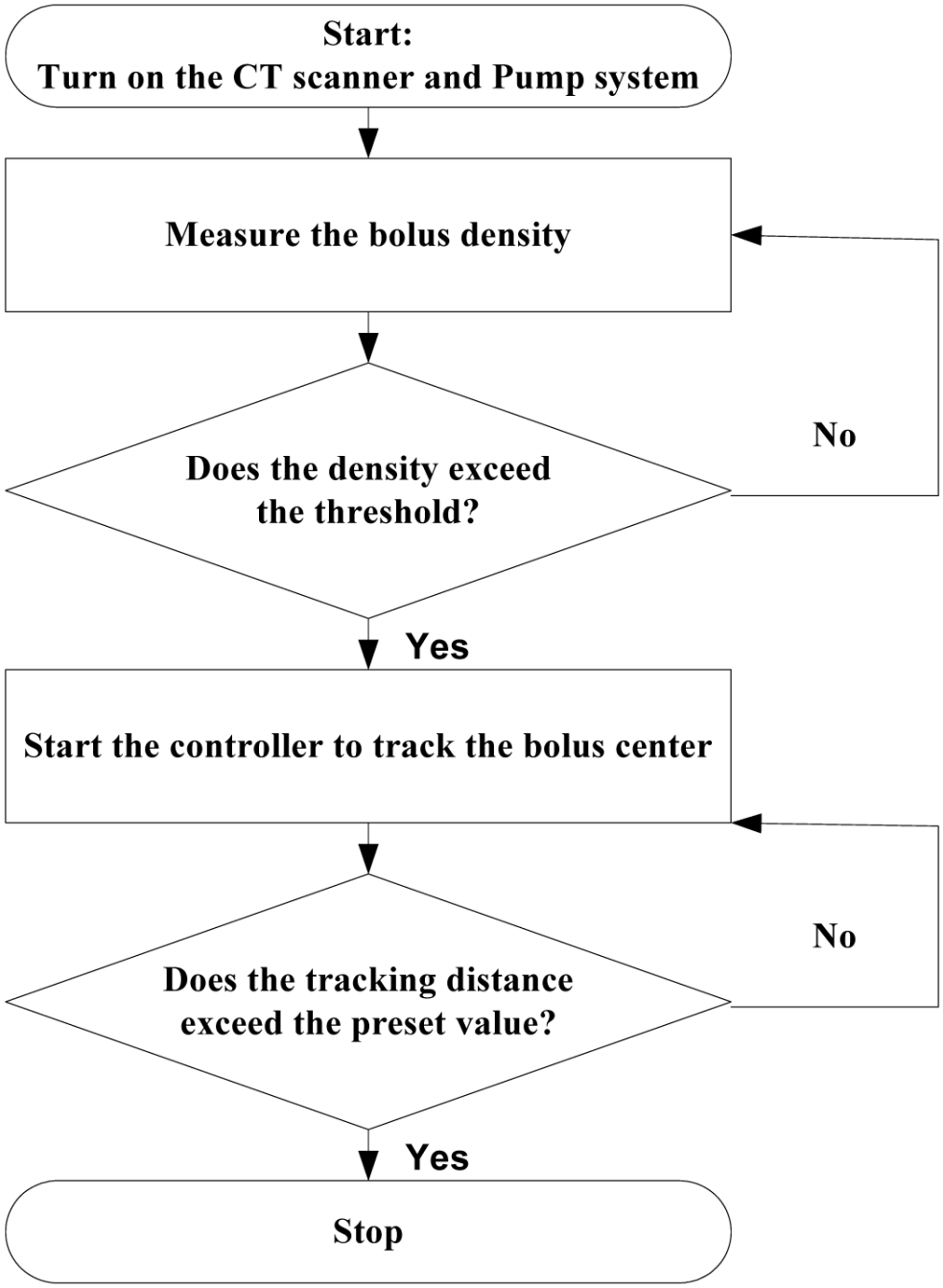

Figure 4. Flow chart of the adaptive bolus chasing procedure

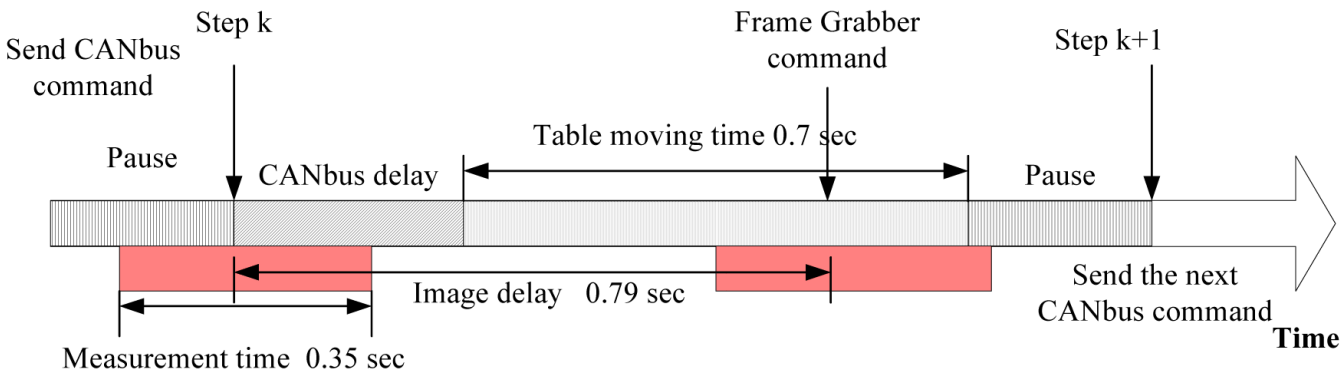

Figure 5. Time arrangement for table moving, waiting and image delay

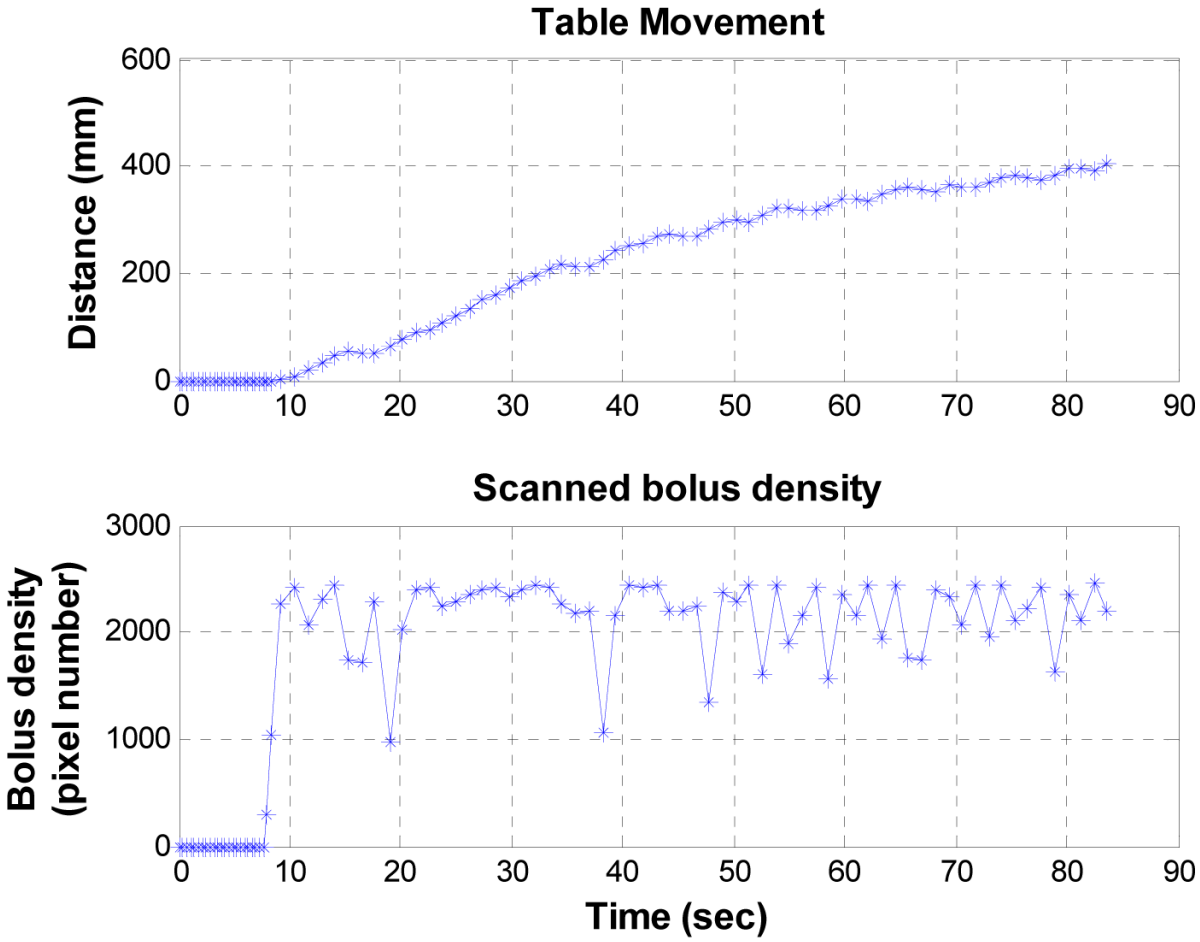

Figure 6. The experimental results for constant pump speed. Top plot: the table position with respect to time; Bottom plot: The scanned bolus density over time

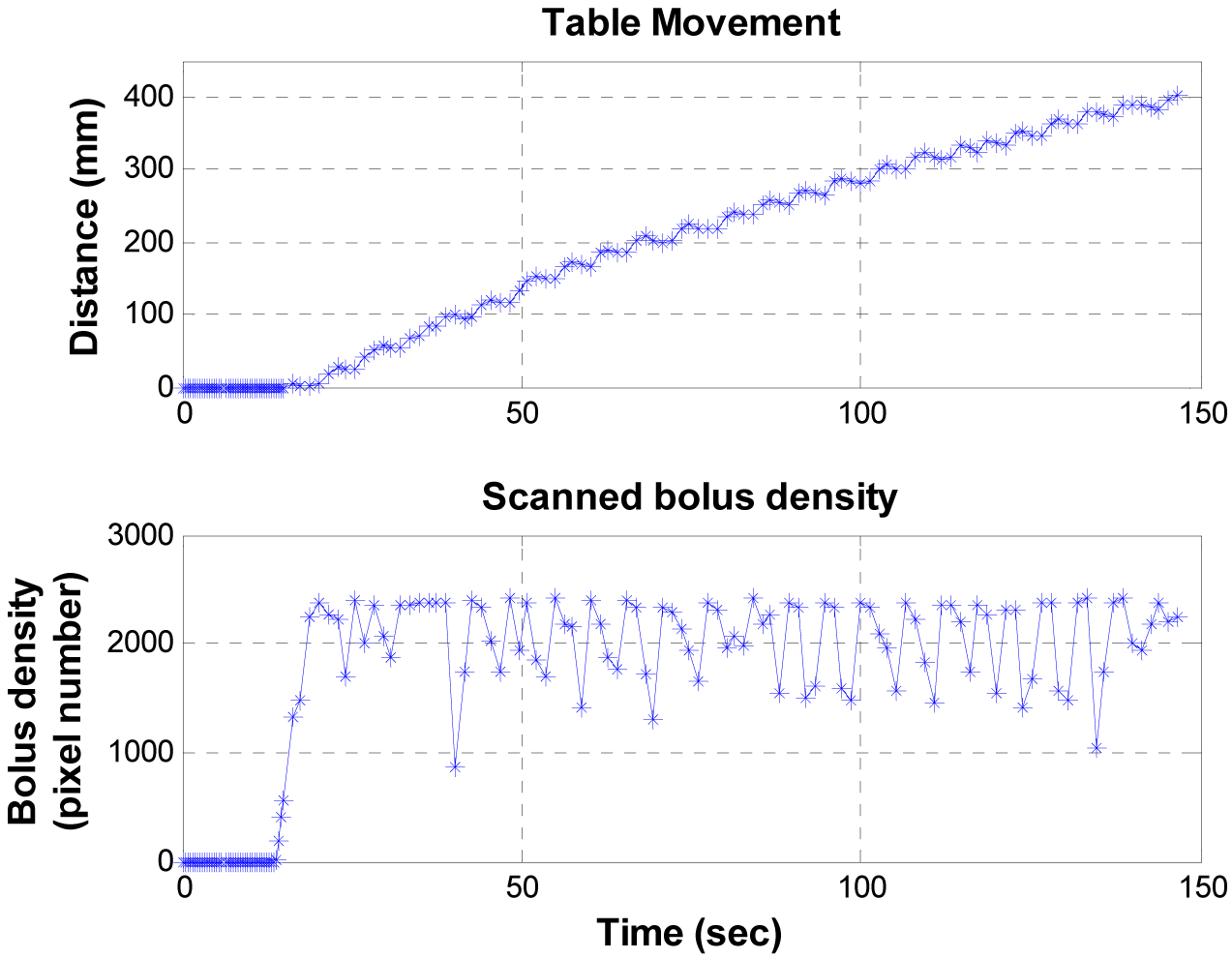

Figure 7. The experimental results for exponentially decreased pump speed. Top plot: the table position with respect to time; Bottom plot: The scanned bolus density over time

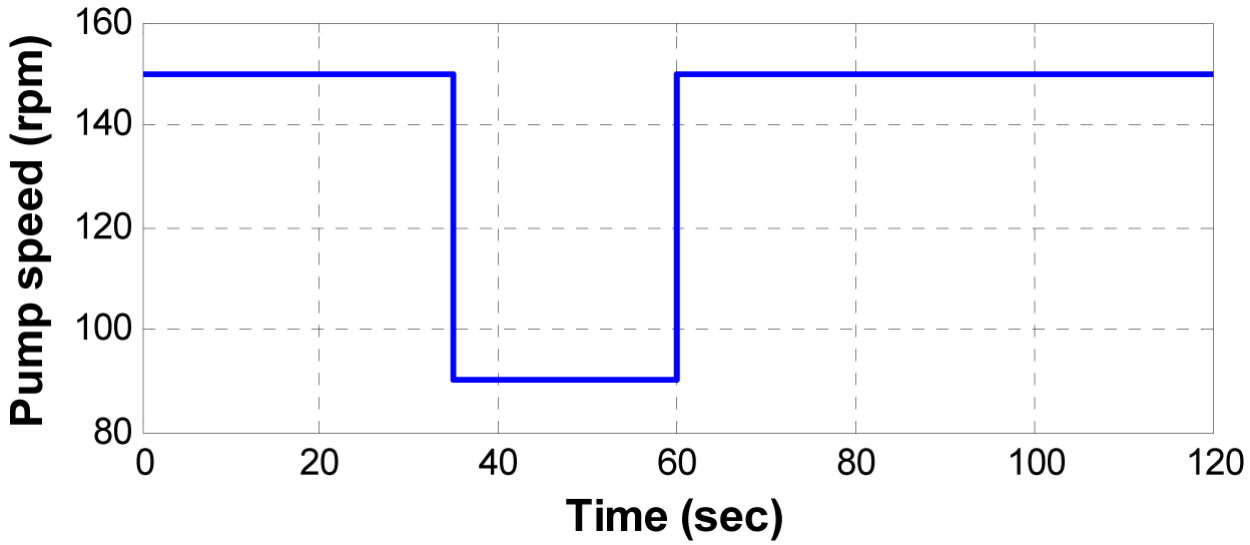

Figure 8. Pump speed for piecewise trajectory

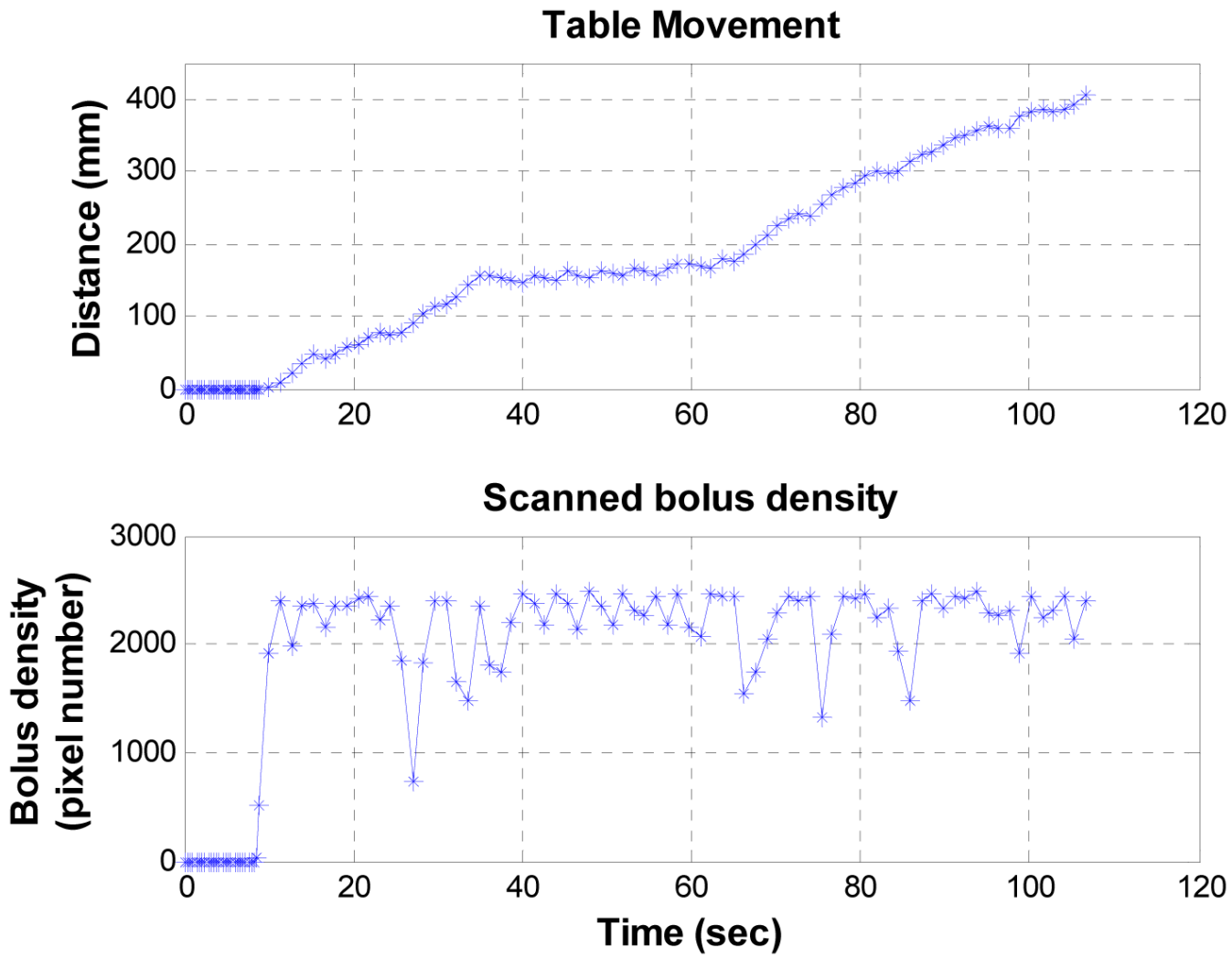

Figure 9. The experimental results for varying pump speed. Top plot: the table position with respect to time; Bottom plot: The scanned bolus density over time

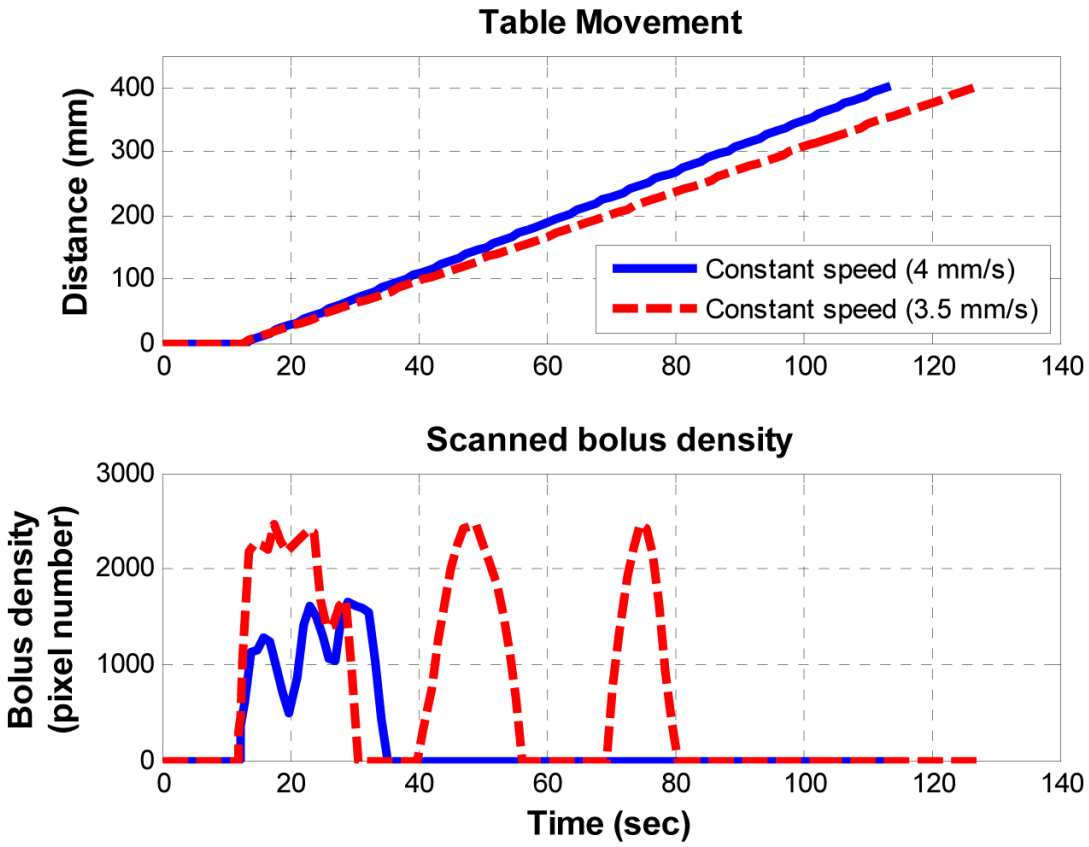

Figure 10. The experimental results for two different constant table speeds (solid line is for 4mm/s and dashed line is for 3.5mm/s). Top plot: the table position with respect to time; Bottom plot: The scanned bolus density over time

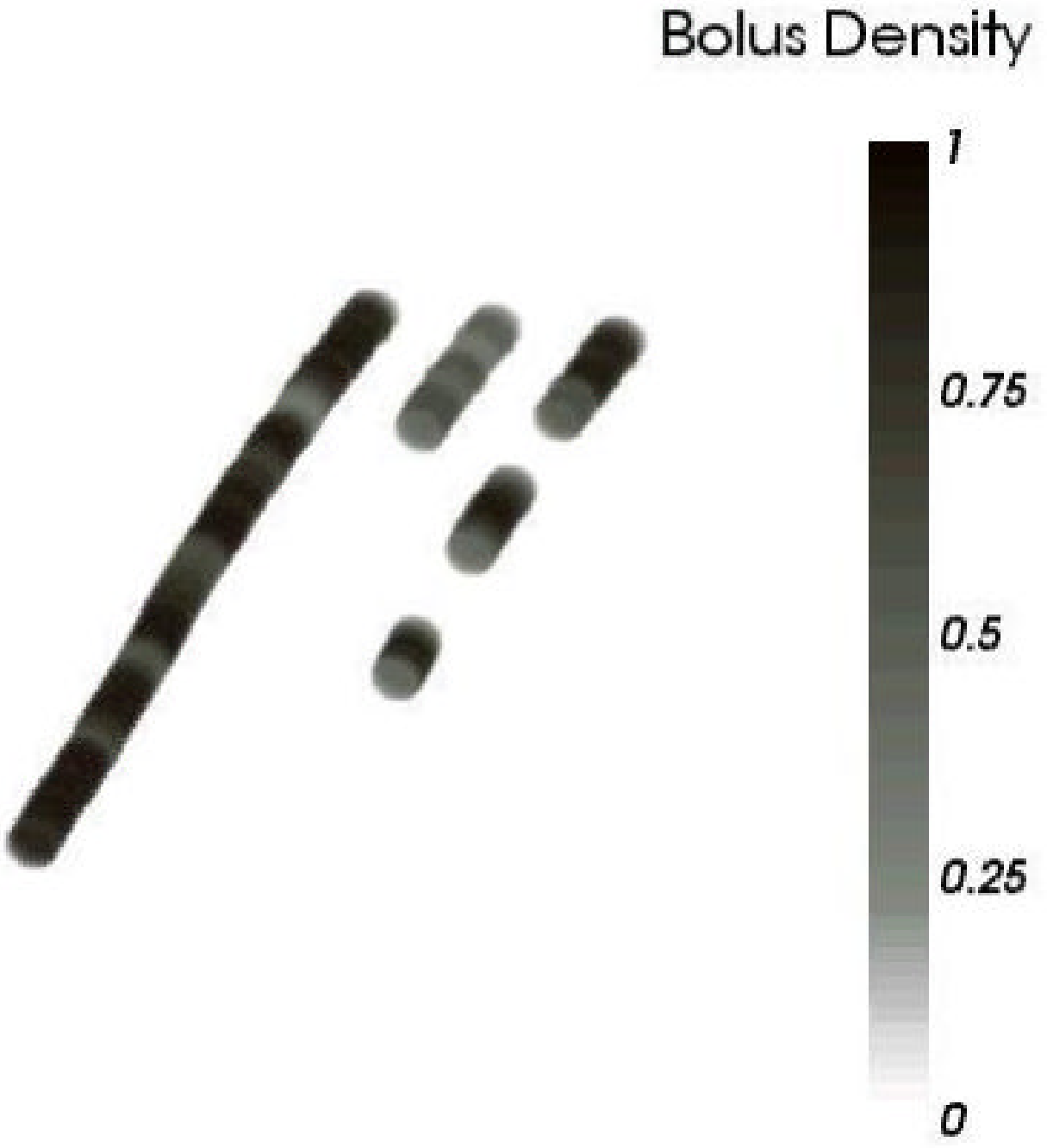

Figure 11. The reconstructed 3D blood vessels of adaptive tracking method (left), 4mm/sec constant speed method (middle), and 3.5mm/sec constant speed method (right)

Table 1

Some technical parameters of the CT scanner

CT table maximum speed	150 mm/sec
Rotation times	0.5s, 0.75s, 1.0s, 1.5s
Slice width	0.5-10mm
Scan field	50cm
Reconstruction field	5-50cm
Monitor resolution	1280 × 1024
Maximum scan length	157cm
Tube voltages	80, 120, 140 kV
Tube current range	28-500mA
Number of projections	1160/2320(1/360°)

Table 2

The scanning and control parameters

Scanning parameters	
Slice	Width: 1.0, collimation: 0.5mm
Voltage	120 kV
Current	81mA
Window	500 HU
Center	1500 HU
FOV (Field of View)	100mm
Center X	-50mm
Center Y	-60mm

Control parameters	
Threshold to start the CT table	500
Alpha $^{\alpha}$	0.25
Variance threshold	200
Delay step *l*	1
Prescribed length	400 mm

Table 3

The averaged scanned density of the adaptive tracking method and the constant speed methods

Method	Adaptive tracking method	4mm/s constant method	3.5mm/s constant method
Average scanned density	2212	260	772
Percentage of the maximum density	88.5%	10.4%	30.9%